DESIGN AND TEST OF A WIRELESS MONITORING SYSTEM FOR FEED RATE IN COMBINE HARVESTER BASED ON BOTTOM PLATE PRESSURE OF CHAIN-RAKE CONVEYOR
/
基于链耙输送器底板压力的联合收割机喂入量无线监测系统设计与试验

Chao ZHANG[*1,2)], Qingling LI[1,2)], Shaobo YE [1,2)], Decong ZHENG[1,2)]
[1)] College of Agricultural Engineering, Shanxi Agricultural University, Taigu 030801, China;
[2)] Key Laboratory of Agricultural Machinery Technology and Equipment of Shanxi Province, Taigu, 030801, China
Corresponding author: Chao Zhang
Tel: +86-139-9457-5375; E-mail: sxndgxyzhangchao@sxau.edu.cn
DOI: https://doi.org/10.35633/inmateh-77-73

Keywords: *Chain-rake conveyor, Bottom plate pressure, Combine harvester, Feed rate*

ABSTRACT
Feed rate is a critical operating parameter in combine harvesters, as it directly influences working efficiency and harvesting quality. To enable real-time and accurate feed rate monitoring, this study proposes a wireless monitoring approach based on pressure measurements at the bottom plate of the chain-rake conveyor inlet. A coupling model relating feed rate, chain-rake speed, and bottom plate pressure was established through theoretical analysis. To enhance robustness against signal fluctuations, the trimean was selected as the feature metric. A monitoring system incorporating LoRa wireless transmission was developed to achieve data acquisition, transmission, and visualization. Bench test results showed that the established model achieved a goodness-of-fit R^2 of 0.9963, and the predictive relative error was below 5% under most working conditions, demonstrating that the system provides high accuracy and stability in complex operating environments. The proposed method offers an effective technical solution for feed rate monitoring in combine harvesters.

摘要
喂入量是联合收获机作业过程中的关键参数，直接影响作业效率与质量。为实现喂入量的实时准确监测，本文提出一种基于链耙输送器入口处底板压力的无线监测方法。通过理论分析建立喂入量、链耙转速与底板压力之间的耦合模型，采用三均值（Trimean）作为鲁棒特征量以抑制信号波动干扰，设计了一套基于 Lora 无线传输的监测系统，实现数据采集、传输与可视化。台架试验结果表明，所建模型拟合优度 R^2 达 0.9963，在多数工况下预测相对误差低于 5%，验证了该监测系统在复杂作业环境下具有良好的准确性与稳定性，为联合收获机喂入量监测提供了有效的技术支撑。

INTRODUCTION
Feed rate is a key operating parameter for grain combine harvesters, directly influencing work quality and efficiency. Insufficient feed rate leads to low equipment load factor, causing energy waste, while excessive feed rate can easily trigger blockages, overloads, and even mechanical damage. Therefore, achieving real-time and precise monitoring of feed rate is of great significance for ensuring efficient and reliable harvesting operations (*Yang et al., 2025*).

Existing feed rate detection methods primarily include machine vision, torque sensing, and pressure sensing. Machine vision methods analyze crop conveying status through image processing (*Zhu et al., 2023; Zhang, 2021*). Torque sensing methods indirectly reflect feed rate by monitoring the load variation of the main shaft (*Wang et al., 2019; Kumhála et al., 2003*). Pressure sensing technology achieves measurement by detecting pressure fluctuations exerted by crops on specific components, offering advantages such as low cost, easy installation, and strong anti-interference capability, making it a current research hotspot (*Chen, 2025*). For instance, an equivalent feed rate model was established using pressure sensors at the chain-rake outlet (*Jie et al., 2009*; *Tang, 2021*) further verified the correlation between pressure and feed rate by combining multi-sensor information. *Putri et al., (2016),* developed a yield monitoring system for rice combine harvesters, integrating microwave flow and moisture sensors with DGPS. The system reliably recorded real-time yield and grain moisture data, with moisture levels reaching up to 26 percent across nearly half of the surveyed area. *Choi et al. (2018)* developed an ultrasonic grain flow sensor for combine harvesters, applicable to rice, soybeans, and barley. Field tests demonstrated strong correlation in yield monitoring for all three crops, indicating significant potential for practical application.

Li et al. (2022), achieved relatively high-precision measurement using header hydraulic cylinder pressure and pointed out the issue of signal interference caused by uneven ground. *Lu (2011)* and *Li (2018)* confirmed the linear relationship between hydraulic pressure and feed rate from the perspectives of the hydraulic continuously variable transmission system and the concave sieve cylinder pressure, respectively. *Sun et al. (2023)*, significantly improved control accuracy using model predictive control and optimization algorithms. Furthermore, *Abdeen (2022)* and *Zhao et al. (2020)* verified the correlation between threshing drum cover stress and feed rate using force-sensing resistors and thin-film sensors, respectively. *Liang (2024)* achieved feed rate prediction using acceleration sensors combined with signal analysis.

However, the aforementioned research mostly focuses on the chain-rake conveyor outlet or the threshing drum area, with relatively little study on the dynamic characteristics of material pressure at the conveyor inlet. The material quantity at the inlet most directly reflects the true feed rate, but signals at this location are susceptible to mechanical vibration and instantaneous material fluctuations, making detection challenging. To address this, this study proposes installing a pressure sensor at the inlet of the chain-rake conveyor, establishing an explicit mathematical model between the inlet bottom plate pressure, feed rate, and speed, and introducing a change-point algorithm for robust signal segmentation, providing a new method for feed rate monitoring and closed-loop control.

MATERIALS AND METHODS

Mathematical Relationship Between Feed Rate and Bottom Plate Pressure

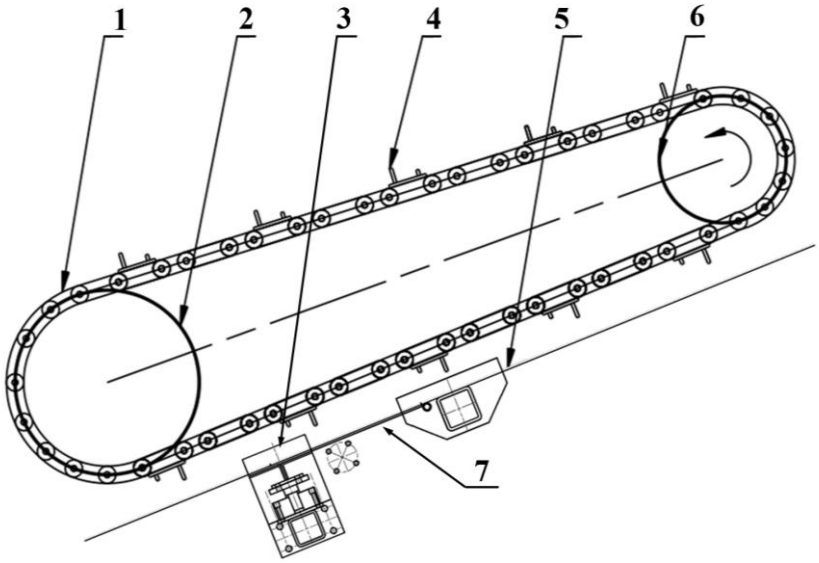

Fig. 1 -Schematic diagram of the chain-rake conveyor and pressure sensor installation structure

1-Conveyor chain; 2-Driven sprocket; 3-Pressure sensor; 4-Rake tooth; 5-rConveyor bottom plate; 6-Drive sprocket; 7-Hinged plate

The structure of the chain-rake conveyor and the bottom plate pressure sensor installation is shown in Fig 1, mainly consisting of the conveyor chain *(1)*, driven sprocket *(2)*, pressure sensor *(3)*, rake teeth *(4)*, conveyor bottom plate *(5)*, drive sprocket *(6)*, and hinged plate *(7)*. During operation, the drive sprocket *(6)* rotates counterclockwise, and the rake teeth *(4)* cooperate with the bottom plate to convey material to the threshing device. The material conveyance rate depends on the chain-rake speed and the material layer thickness, whose variation causes changes in the pressure on the bottom plate.

To establish a theoretical model, this study takes mature maize stalks (moisture content approx. 28%) as the object, treating them as transversely isotropic compressible materials. Assuming the initial radius of a single stalk is r_0, the compressed radius is r_1 (compression ratio $\beta=(r_0/r_1)^2>1$), and the axial length L is constant. The chain-rake action time t_c is inversely proportional to the conveyor chain speed w_b:

$$t_c = \kappa/\omega_b \tag{1}$$

where κ is a geometric constant related to the rake tooth pitch.

The feed rate Q_m (kg/s) determines the number of stalks N compressed per unit time:

$$N = \frac{Q_m}{\rho_0 V_0} = \frac{Q_m}{\rho_0 \pi r_0^2 L} \tag{2}$$

where ρ_0 is the initial density of the straw, V_0 is the volume of a single straw stalk, and L is the axial length of a single straw stalk.

During the compression process, the dynamic deformation behavior of the material must be considered. The volumetric true strain rate $\dot{\varepsilon}_v$ is characterized as:

$$\dot{\varepsilon}_v = \frac{\varepsilon_v}{t_c} = \frac{\ln \beta}{\kappa}\omega_b \tag{3}$$

where $\varepsilon_v = ln(V_0/V_1) = \ln \beta$ is the amplitude of the volumetric strain.

The rheological behavior of corn stalks is described using a Cowper-Symonds type power-law model, where the dynamic term dominates (*Ma et al., 2016*):

$$\sigma = \sigma_0[1 + \left(\frac{\dot{\varepsilon}_v}{D}\right)^m] \approx K\dot{\varepsilon}_v{}^m \tag{4}$$

where: σ is Dynamic compressive stress (Pa); K =σ_0/D_m is Strain rate sensitivity coefficient; m is Strain rate hardening exponent.

The floor pressure is generated by the coupling of the dynamic stress per straw stalk and the flow rate. The average contact area per straw stalk A_c can be expressed as:

$$A_c = \xi \pi r_0 L \tag{5}$$

where ξ is a shape factor. The contact force on a single straw stalk F_{stalk} is:

$$F_{stalk} = \sigma A_c = \xi \pi r_0 LK(\frac{\ln \beta}{\kappa}\omega_b)^m \tag{6}$$

The total pressure for compressing N stalks per unit time is:

$$P_{total} = NF_{stalk} = \frac{Q_m}{\rho_0 \pi r_0^2 L}\xi \pi r_0 LK(\frac{\ln \beta}{\kappa}\omega_b)^m \tag{7}$$

Considering the relationship $r_1^2/r_0^2 = 1/\beta$, and consolidating constants related to material properties and geometry into a single parameter, the expression can be simplified to a form showing the coupling between feed rate Q_m and rotational speed ω:

$$P_{total} = C_m Q_m \omega_b{}^m \tag{8}$$

The constants C_m and the exponent m can be determined through bivariate experiments. Simultaneously, it can be observed from the formula that a larger feed rate results in greater floor pressure; a higher chain-rake rotational speed ω also significantly increases the floor pressure. This coupling relationship provides the theoretical foundation for the subsequent real-time monitoring of feed rate.

Construction of the Wireless Feed Rate Monitoring System

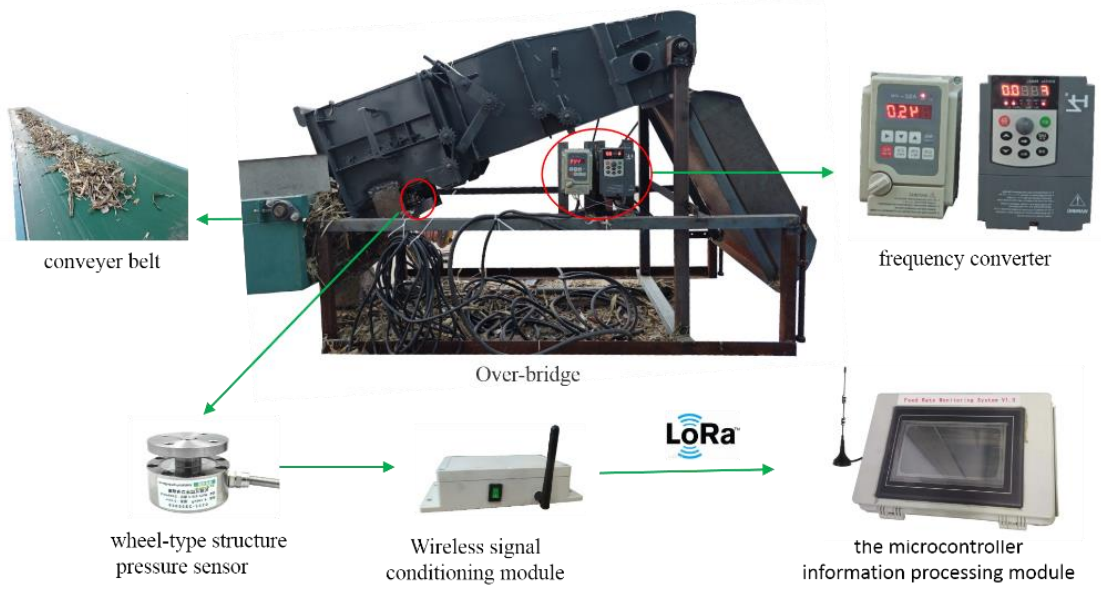

Fig. 2 - Overall architecture of the detection system

Based on a Kubota 688 combine harvester platform, a wireless feed rate monitoring system was designed as shown in Fig 2, including mechanical transmission, sensing detection, signal conditioning, and wireless transmission units. The mechanical transmission part is driven by a three-phase asynchronous motor to operate the conveyor chain and belt, with precise speed control via a frequency converter to simulate different feed conditions.

Fig. 3 - Pressure sensor installation diagram

In the sensing detection unit, a square opening was pre-machined on the bridge bottom plate. The removed section was hinged to the original plate via hinges, forming a flexibly openable hinged plate assembly. A spoke-type pressure sensor (as shown in Fig 3) with a range of 0~300 kg was installed centrally beneath this hinged plate, using a 4-wire connection to reduce the influence of lead resistance. The analog voltage signal collected by the sensor is processed by a self-made wireless signal conditioning module. Data is framed following the standard Modbus-RTU communication protocol and transmitted wirelessly to the microcontroller signal processing module located at the display terminal. The microcontroller system is responsible for parsing, computing, and storing the data packets.

To simplify system wiring and improve assembly flexibility, this solution employs LoRa wireless communication technology for data transmission. LoRa, based on spread spectrum frequency-hopping modulation, offers large network capacity, high reliability, and low-power long-distance transmission characteristics, and is now widely used in farmland information monitoring and smart irrigation systems. Specifically, LoRa modules developed by Zhengdian Atomic were used, with the core being the Semtech SX1278 chip, supporting 32 configurable channels. The LoRa module communicates with the microcontroller (STM32C8T6) via a serial port. The circuit schematic of the self-made wireless signal conditioning module is shown in Fig 4.

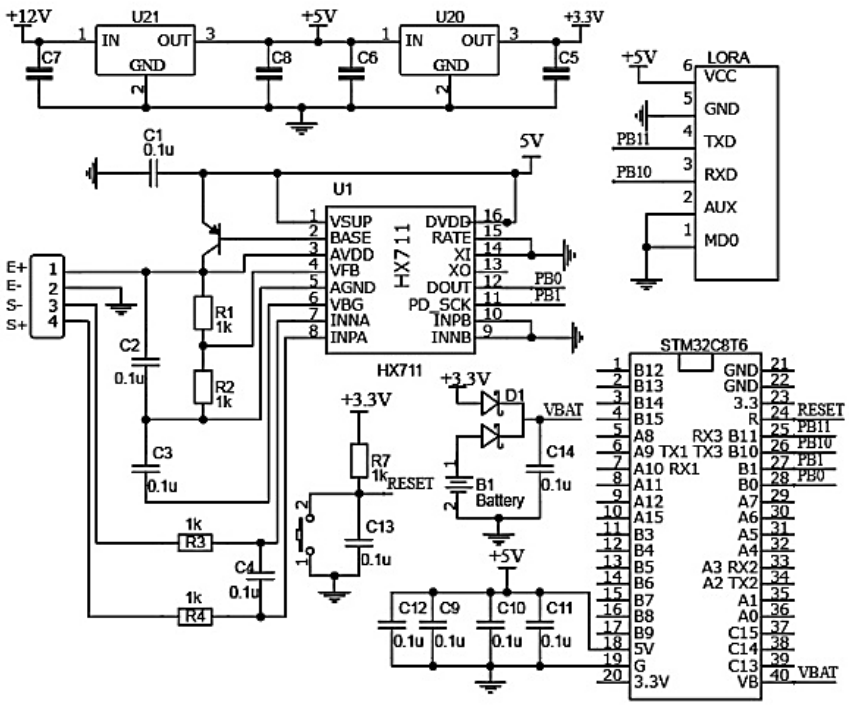

Fig. 4 - Hardware circuit diagram of the wireless signal conditioning module

The receiving end LoRa module uses the same serial port parameter configuration as the transmitting end. The display screen selected was an HMI80480KM070 resistive serial screen produced by Guangzhou Dacai Photoelectric Technology Co., Ltd., with the host computer interface developed based on the VisualHMI platform. Since this serial screen uses the RS-232 Level standard, while the microcontroller output is TTL level, a MAX232 chip from Maxim Integrated was used for level conversion. An SD card was used as the data storage medium. The hardware circuit of the microcontroller signal processing module is shown in Fig. 5.

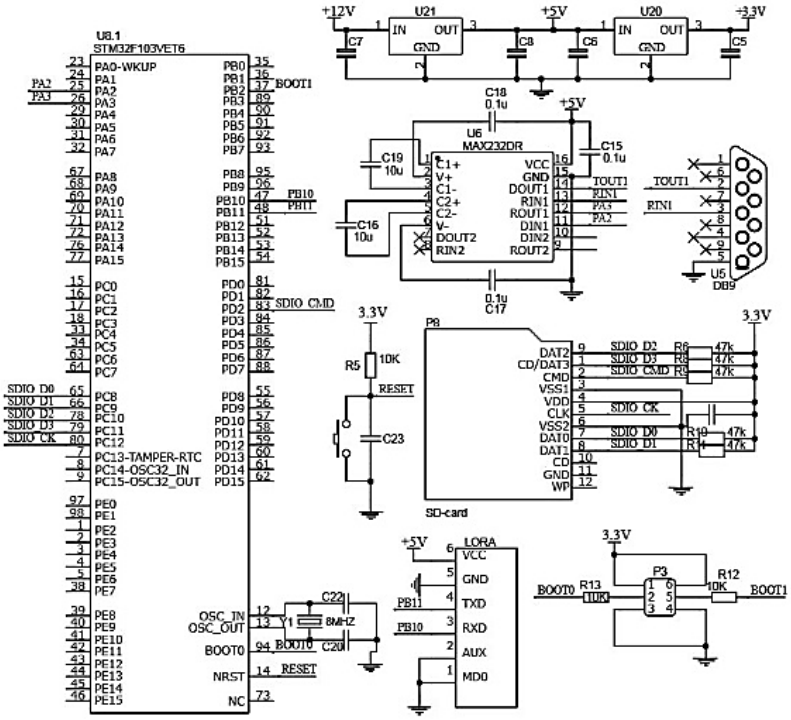

Fig. 5 - Hardware circuit diagram of the microcontroller signal processing module

The microcontroller program was written using Keil μVision5 to achieve Modbus RTU data interaction with the wireless module, DCBUS protocol communication with the serial screen, and SD card storage management. Modular programming was adopted to enhance maintainability.

RESULTS

To evaluate system performance, bench tests were conducted under different feed rates and chain-rake speeds. A typical pressure response curve is shown in Fig 6, which can be divided into three stages: no-load (Stage 1), feeding (Stage 2), and unloading (Stage 3). The Stage 2 pressure signal rises significantly with fluctuations, directly reflecting the variation in feeding load. However, due to factors such as the initial state of the material and preload force, the signal baseline exhibits some fluctuations.

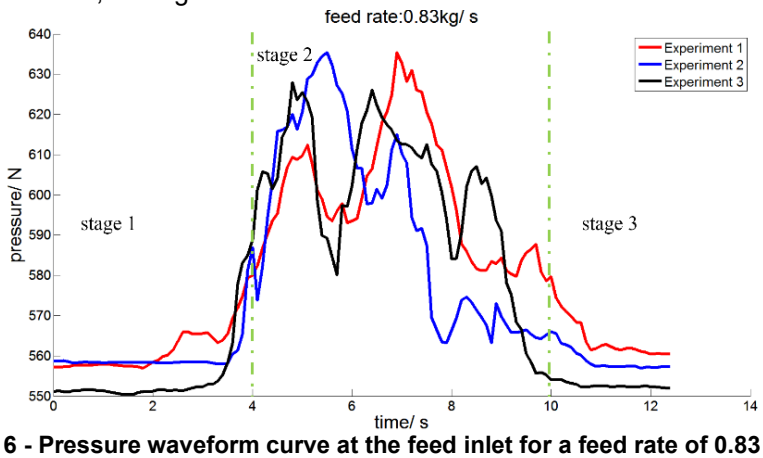

Fig. 6 - Pressure waveform curve at the feed inlet for a feed rate of 0.83 kg/s

To further establish a quantitative relationship between bottom plate pressure and feed rate, it is necessary to extract highly robust feature parameters from Stage 2. Traditional methods often use the arithmetic mean or median as representative values.

However, during the actual operation of combine harvesters, pressure signals often contain abnormal fluctuations due to uneven material flow, mechanical vibration, and external interference, making the mean and median sensitive to outliers and affecting model accuracy.

To address this issue, this paper introduces the trimean as a new statistical feature to describe the Stage 2 pressure distribution. Its calculation formula is as follows:

$$T = \frac{(Q1+2Q2+Q3)}{4} \tag{9}$$

where $Q1$, $Q2$, and $Q3$ represent the first quartile, median, and third quartile of the sample, respectively.

To systematically evaluate the superiority of the trimean in practical applications, this paper conducted feature extraction and comparative analysis under multiple repeated experimental conditions for Stage 2 data. Three sample statistics—mean, median, and trimean—were calculated, and statistical indicators such as the coefficient of variation were introduced for comparison. Specific experimental results are shown in Table 1 and Fig 7. From the statistical results, it can be seen that the trimean exhibited a lower coefficient of variation (10.56%) and range (9.16) compared to the mean and median in repeated trials, demonstrating better stability and more reliably reflecting the pressure response characteristics under a fixed feed rate.

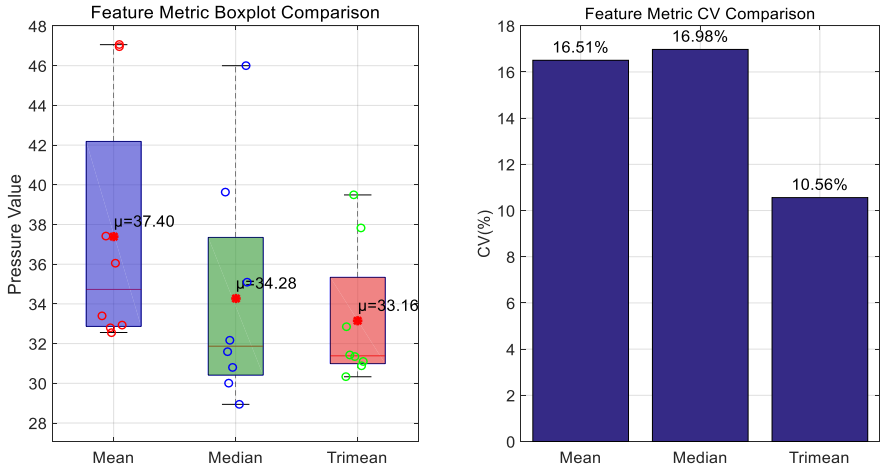

Fig. 7 - Box plots and comparison of coefficients of variation for mean, median, and trimean

Table 1

Experimental statistics of mean, median, and trimean under multiple repeatability test conditions

No.	1	2	3	4	5	6	7	8
Mean / N	33.41	32.56	37.42	47.06	32.8	32.94	46.95	36.05
Median / N	31.58	35.08	32.16	46	30.02	30.81	39.62	28.94
Trimean / N	31.43	32.84	31.09	39.49	30.89	31.34	37.84	30.33

Based on the aforementioned signal processing and feature extraction, this study systematically collected pressure data from the chain-rake conveyor bottom plate under various operating conditions. Tests were set up with combinations of different feed rates (0.28~0.83 kg/s) and chain-rake speeds (347~490 r/min). Each condition was repeated 3 times, and the pressure trimean of Stage 2 was extracted as the representative feature. The results are summarized in Tables 2 and 3.

Table 2

Experimental trimean pressure values under different feed rates (chain-rake speed 400 r/min)

Feed rate (kg/s)	Pressure-Exp 1 (N)	Pressure-Exp 2 (N)	Pressure-Exp 3 (N)	Pressure-mean (N)
0.83	60.61	52.36	41.37	51.45
0.56	32.96	35.54	33.39	33.96
0.42	23.64	24.08	26.08	24.6
0.33	18.48	17.82	23.38	19.89
0.28	13.68	14.75	18.07	15.5

Table 3

Experimental trimean pressure values under different chain-rake speeds (feed rate 0.83 kg/s)

Speed (r/min)	Pressure-Exp 1 (N)	Pressure-Exp 2 (N)	Pressure-Exp 3 (N)	Pressure-mean (N)
347	34.26	37.39	54.2	41.95
382	56.21	35.82	51.0	47.68
415	50.7	53.38	60.65	54.91
457	71.38	53.93	63.78	63.03
490	81.59	72.41	45.34	66.44

To scientifically evaluate the significance of the effects of feed rate and chain-rake speed on bottom plate pressure, one-way analysis of variance (ANOVA) was performed for each factor, with results shown in Tables 4 and 5.

Table 4

ANOVA table for feed rate

Source of Variation	SS	Df	MS	F-value	p-value
Between Groups	2439.01	4	609.75	27.40	<0.001
Within Groups	222.51	10	22.25		
Total	2661.52	14			

From Table 4, the F-value for feed rate is 27.40, much greater than the critical value F(4,10) = 3.48 at the α=0.05 significance level, and the p-value is less than 0.001, indicating that feed rate has an extremely statistically significant effect on bottom plate pressure. Combined with the data in Table 2, it can be further observed that as the feed rate decreases from 0.83 kg/s to 0.28 kg/s, the average pressure drops from 51.45 N to 15.50 N, showing a clear positive correlation trend. This suggests that an increase in feed rate directly leads to an increase in bottom plate pressure.

Table 5

ANOVA table for chain-rake speed

Source of Variation	SS	Df	MS	F-value	p-value
Between Groups	1257.75	4	314.44	2.29	0.12
Within Groups	1370.89	10	137.09		
Total	2628.64	14			

Although the data in Table 3 shows that when the feed rate is fixed at 0.83 kg/s, the average pressure increases from 41.95 N (347 r/min) to 66.44 N (490 r/min) with increasing chain-rake speed, the ANOVA results (Table 5) show an F-value of 2.29, which is less than the critical value F(4,10)=3.48, and a p-value of 0.12, greater than the 0.05 significance level. This indicates that the effect of chain-rake speed on pressure did not reach statistical significance under the experimental conditions. The main reason is the large within-group variation and poor data consistency under high-speed conditions (e.g., 490 r/min), causing the speed effect to be masked by error.

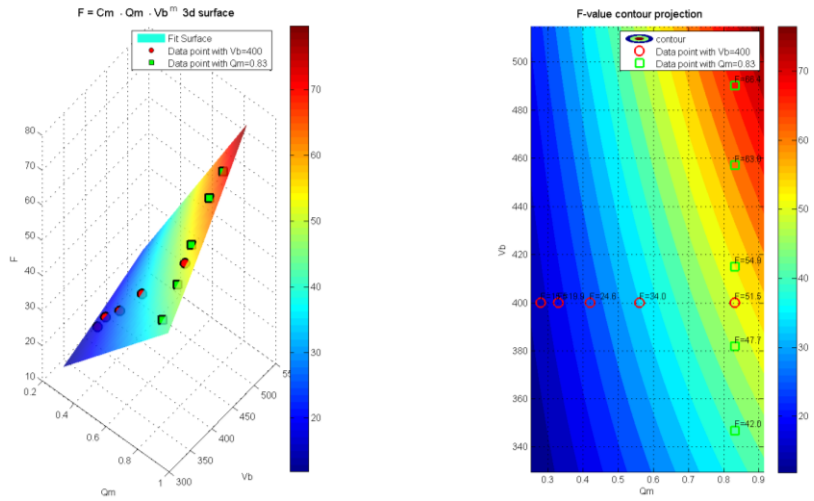

Fig. 8 - 3D surface plot and contour projection plot

Based on the theoretical model, parameters were estimated using nonlinear least squares fitting, yielding C_m = 0.0156 and m = 1.3823. The sum of squared errors (SSE) was 10.5636, and the coefficient of determination R^2 = 0.9963, indicating that the model has extremely high explanatory power for the experimental data. The 3D surface and contour projection plots shown in Fig 8 further visually reflect the high consistency between predicted and measured values.

Table 6 lists the theoretical predicted values, measured values, and relative errors for bottom plate pressure under different combinations of feed rate and chain-rake speed. It can be seen that for most working conditions, the model's predictive relative error is below 5%. Only at a feed rate of 0.28 kg/s is the relative error larger (10.20%). The reason may be that the material layer thickness is thinner under low feed rates, leading to a lower signal-to-noise ratio for the sensor signal, where minor disturbances are easily amplified. Nevertheless, considering the overall error distribution, the established model still has high predictive accuracy and engineering applicability.

Table 6

Comparison of theoretical predicted pressure values with measured values and error analysis

Feed rate (kg/s)	Speed (r/min)	Theoretical pressure	Measured pressure	Relative error (%)
0.83	400	51.17	51.45	0.55%
0.56	400	34.53	33.96	1.65%
0.42	400	25.89	24.6	4.98%
0.33	400	20.35	19.89	2.26%
0.28	400	17.26	15.5	10.20%
0.83	347	42.04	41.95	0.21%
0.83	382	48.02	47.68	0.71%
0.83	415	53.84	54.91	1.99%
0.83	457	61.52	63.03	2.45%
0.83	490	67.74	66.44	1.92%

CONCLUSIONS

This study designed and implemented a wireless monitoring system for feed rate in combine harvesters based on the bottom plate pressure of the chain-rake conveyor. Through theoretical modeling, hardware design, and experimental verification, the following conclusions were drawn:

(1) A nonlinear coupling model between feed rate, chain-rake speed, and bottom plate pressure was established. Parameter identification results showed that this model has high predictive accuracy (R^2=0.9963) and is suitable for real-time estimation of feed rate.

(2) The trimean was introduced as a feature extraction method for the pressure signal, effectively suppressing interference from abnormal fluctuations and significantly improving the stability and robustness of the feature quantity.

(3) The developed wireless monitoring system, based on LoRa communication technology, features easy installation, strong anti-interference capability, and reliable transmission, making it suitable for long-term stable operation in complex field environments.

(4) Feed rate had a significant effect on bottom plate pressure ($p<0.001$), whereas the chain rake speed did not demonstrate statistical significance under the experimental conditions.

This study provides a low-cost, high-precision solution for real-time monitoring and intelligent control of feed rate in combine harvesters, with good prospects for engineering application. Subsequent work could optimize sensor placement, introduce multi-sensor fusion methods, and conduct field validation to enhance system adaptability.

ACKNOWLEDGEMENT

This research was funded by Special project for Discipline Construction of Shanxi Agricultural University in 2025 (Research and development of multi-source sensing of buckwheat harvester feeding amount and CVT electro-hydraulic control system of threshing drum), the Scientific and Technological Innovation Programs of Higher Education Institutions in Shanxi (No.2022L096) and the Youth Science and Technology Innovation Project of Shanxi Agricultural University (No.2020QC12).

REFERENCES

[1] Abdeen M., Xie G., Salem A., Fu J., Zhang G., (2022). Longitudinal axial flow rice thresher feeding rate monitoring based on force sensing resistors. *Scientific reports*, Vol. 12, Issue 1, 1369. https://doi.org/10.1038/s41598-021-04675-w.

[2] Chen X., (2025). Research on the feeding rate detection technology of combine harvester based on the force exerted by the reel on wheat plant（基于拨禾轮对小麦植株作用力的联合收获机喂入量检测技术研究）(Doctor's thesis). *Henan Agricultural University,* Zhengzhou / China, https://doi.org/10.27117/d.cnki.ghenu.2025.000002.

[3] Choi, M., Lee, K., Jang, B, Kim, Y., Chung, S., Lee, J., Kim, S., (2018). Grain flow rate sensing for a 55 kW full-feed type multi-purpose combine. *International Journal of Agricultural and Biological Engineering*, Vol. 11, Issue 5, pp. 206-210. DOI: https://doi.org/10.25165/j.ijabe.20181105.2686.

[4] Jie Z., Luo S., Zhou X., (2009). LabVIEW-based telemetering experiments of rice feed quantity for combined harvester（基于 LabVIEW 的联合收割机水稻喂入量遥测试验）. *Transactions of the CSAE,* Vol.25, Issue S2, pp.87-91.

[5] Kumhála F. & Prošěk V., (2003). Laboratory Measurement of Mowing Machine Material Feed Rate. *Precision Agriculture,* Vol.4, Issue4, pp. 413-419, DOI:10.1023/A:1026327509618.

[6] Li P., Cui J., Feng W., Zhang X., Zhang T., Li Y., (2022). Design and Test of real-time Monitoring System for Feeding Quantity of Small Combine（小型联合收割机喂入量实时监测系统设计与试验）. *Journal of Agricultural Mechanization Research,* Vol. 44, Issue 9, pp. 240-246. https://doi.org/10.13427/j.cnki.njyi.2022.09.031.

[7] Li Y., Wang J., Xu L., Tang Z., Xu Z., Wang K., (2018). Design and Experiment on Adjusting Mechanism of Concave Clearance of Combine Harvester Cylinder (联合收获机脱粒滚筒凹板间隙调节装置设计与试验). *Transactions of the Chinese Society for Agricultural Machinery*, Vol. 49, Issue 8, pp. 68-75.https://doi.org/ 10.6041/j.issn.1000-1298.2018.08.008.

[8] Liang Z., Qin Y., Su Z., (2024). Establishment of a Feeding Rate Prediction Model for Combine Harvesters[J]. *Agriculture Basel*, Vol. 14, Issue 4, pp. 589, DOI:10.3390/agriculture14040589.

[9] Lu W., Liu B., Zhang D., Li J., (2011). Experiment and Feed Rate Modeling for Combine Harvester (谷物联合收获机喂入量建模与试验). *Transactions of the Chinese Society for Agricultural Machinery*, Vol. 42, Issue S1, pp. 82-85.

[10] Ma Y., Xuan C., Wu P., Yang J., Su H., Zhang Y., (2016). Designing a real-time feed measurement system for horizontal axial flow threshing drum based on thin film sensor（玉米秸秆振动压缩过程的应力松弛试验）. *Transactions of the Chinese Society of Agricultural Engineering (Transactions of the CSAE),* Vol. 32, Issue 19, pp. 88-94. DOI: https://doi.org/10.11975/j.issn.1002-6819.2016.19.012.

[11] Putri, R., Yahya, A., Adam, N., Aziz, S., (2016). Performance evaluation of yield monitoring system for rice combine harvester in Selangor, Malaysia. *International Journal on Advanced Science Engineering Information Technology*, Vol. 6, Issue1, pp. 35-39. DOI: https://doi.org/10.18517/ijaseit.6.1.612.

[12] Sun Y., Liu R., Li S., Zhang M., Li H., (2023). Feed Rate Control Method and Simulation Experiment of Combine Harvester Based on GWO-MPC *(基于 GWO-MPC 的联合收获机喂入量控制方法与仿真实验).* *Transactions of the Chinese Society for Agricultural Machinery*, Vol. 54, Issue 11, pp. 83-91. https://doi.org/ 10.6041/j.issn.1000-1298.2023.11.008.

[13] Tang L., (2021). Design of Combine Harvester Feeding Rate Detection System and Research on the Detection Method. *（联合收割机喂入量检测系统设计及检测方法研究）*(Master's thesis). *Jiangsu University*. Zhenjiang/China. https://doi.org/10.27170/d.cnki.gjsuu.2021.000881.

[14] Wang S., Hu Z., Wu F., Yu Z., Cao M., Gao X., (2019). Modeling and experiment of feeding rate for full-feed peanut pickup harvester (全喂入花生捡拾收获机喂入量建模与试验). *Transactions of the Chinese Society of Agricultural Engineering (Transactions of the CSAE),* Vol.35, Issue23, pp.29-36, https://doi.org/10.11975/j.issn.1002-6819.2019.23.004.

[15] Yang X., Li P., Zhao Z., Lei C., Jin C., (2025). A review of the feed rate detection and stability control methods in combine Harvesters, *INMATEH–Agricultural Engineering,* Vol.75, Issue1, pp.143-157, DOI: https://doi.org/10.35633/inmateh-75-12.

[16] Zhao S., Zhang G., Zhang S., Fu J., Xie G., Mohamed A., (2020). Designing a real-time feed measurement system for horizontal axial flow threshing drum based on thin film sensor(基于薄膜传感器的横轴流脱粒滚筒实时喂入量测量系统设计), *Journal of Huazhong Agricultural University,* Vol. 39, Issue 02, pp. 160-169. https://doi.org/10.13300/j.cnki.hnlkxb.2020.02.020.

[17] Zhang S. Q. (2021). Monitoring the feeding quantity and quality of rape harvest based on machine vision *(基于机器视觉的油菜收获喂入量及品质监测)* (Master's thesis). *Nanjing University,* Nanjing/China. https://doi.org/10.27235/d.cnki.gnjiu.2021.000752.

[18] Zhu L., Xu M., Wang A., Zhang D., Qian W., Li C., (2023). *Research on rice growth density detection at maturity stage based on improved DeepLabV3+ (基于改进 DeepLabV3+的成熟期水稻生长密度检测研究). Journal of Chinese Agricultural Mechanization,* Issue 44, pp.186-192, 209, https://doi.org/10.13733/j.jcam.issn.2095-5553.2023.12.028.